



Cite this: *Sustainable Food Technol.*, 2025, 3, 1203

## Cold plasma enhanced gelation and thermal properties of oat protein and its application in a selected model food system

Gunaseelan Eazhumalai, Ranjitha Gracy T. K. and Uday S. Annapure \*

Cold plasma-induced reactions are anticipated to yield structural changes in plant proteins to desirably modify their gelation properties. The present study aimed to investigate the effects of atmospheric pin-to-plate cold plasma treatment on the gelation and thermal properties of oat protein. Oat protein was subjected to cold plasma at different input voltages (170 V and 230 V) and exposure times (15 min and 30 min) and was studied for its rheological and thermal characteristics. Protein gels were made using the thermal gelation method at the lowest gelation concentration (20% w/v) and were studied for their rheological and textural properties. While all the plasma-treated protein dispersions showed increased rheological properties due to the induced aggregation, the gels formed from the 230 V-15 min treated sample exhibited higher viscosity (~7981 cP), visco-elastic moduli ( $G'$  – 3682.4 Pa;  $G''$  – 1170.50 Pa) and stability ( $\gamma_c$  – 2.11%) compared to all other samples owing to the medium-sized aggregates and the positive zeta potential. This might also be attributed to a decreased denaturation temperature (~93.29 °C) of the sample. Additionally, plasma-treated oat protein-incorporated patties demonstrated improved functional properties, including reduced syneresis loss (~74% reduction) and increased compression juice loss (~36% rise) due to enhanced moisture retention and water holding capacity. Textural analysis revealed that patties containing oat protein treated at 230 V for 15 min exhibited superior softness after cooking. These findings suggest that cold plasma treatment enhances the gelation properties of oat protein under specific treatment conditions, improving the textural attributes of the plant-based patties.

Received 1st April 2025

Accepted 4th June 2025

DOI: 10.1039/d5fb00129c

rsc.li/susfoodtech

### Sustainability spotlight

The study titled, 'Cold plasma enhanced gelation and thermal properties of oat protein and its application in a selected model food system' deals with a non-thermal processing technology as a solution to modify a sustainable protein. The use of cold plasma to modify plant protein aligns with multiple UN Sustainable Development Goals (SDGs) by promoting sustainable food innovation. It supports SDG 9 (Industry, Innovation & Infrastructure) through non-thermal, eco-friendly processing of plant-based protein options as an alternative to animal proteins; SDG 13 (Climate Action) benefits from the reduced carbon footprint of plant proteins as the technology is a green zero residue discharge process and SDG 15 (Life on Land) is supported by reducing deforestation caused by livestock farming.

## 1. Introduction

The rising demand for plant-based meat alternatives has driven extensive research into the functional properties of plant-derived proteins.<sup>1</sup> The market demand for plant proteins was approximately 14.3 billion USD in the year 2024 and is anticipated to grow at a compound annual growth rate (CAGR) of 7.5%, reaching 20.5 billion USD by 2029.<sup>2</sup> Given the growing market for plant-based meat alternatives, there is a pressing need to explore innovative and sustainable approaches to extract and enhance the functional properties of plant proteins. Among the many sources including wheat, soy, pea, rice, potato,

and beans, oat protein has recently garnered attention due to its balanced amino acid composition, hypoallergenic nature, and sustainability.<sup>3</sup> The structural similarity between oat protein 12S globulin and soy protein 11S glycinin highlights the potential of oat protein as a substitute for soy protein.<sup>4</sup> However, its limited solubility, gelation, emulsification, and binding abilities pose significant challenges in its application as a structuring agent in plant-based products.<sup>5</sup> Enhancing the gelation properties of oat protein through modification processes could significantly improve its performance in plant-based products, providing a clean-label and allergen-free alternative.

Cold plasma (CP) treatment, a non-thermal processing technology, has emerged as a promising approach for modifying protein structure and improving its functional properties.

Institute of Chemical Technology, Mumbai, India. E-mail: us.annapure@ictmumbai.edu.in



Cold plasma is a partially ionized gas comprising free radicals, energized ions, atoms, and reactive species which tend to interact with exposed components to attain energetic stability.<sup>6</sup> CP treatment has been reported to alter the physicochemical properties of plant proteins, enhancing solubility, emulsification, and gelation. Previous studies have demonstrated that CP treatment can effectively modify soy,<sup>7</sup> pea,<sup>8</sup> and peanut proteins,<sup>9</sup> improving their functionality. However, studies investigating protein modification techniques often lack comprehensive evaluations of their effects in real food systems. While some of these cited studies explored the structural changes induced by CP in plant proteins, there is a critical gap in understanding how these modifications translate to improved textural and sensory attributes in plant-based food formulations. The authors of the present study have already elaborately studied the effect of pin-to-plate cold plasma on the structural, chemical, and foaming characteristics which was the first study on cold plasma modification of oat protein.<sup>10</sup> However, there is a lack of research on the impact of CP treatment on oat protein in the context of its gelation behavior and application in a real-time food system. Thus, this study aims to bridge this gap by investigating the effect of CP treatment on the gelation properties of oat protein and evaluating its application as a binder in plant-based patties. By assessing changes in protein thermo-gelation characteristics, and textural and functional performance in a model food system, this research will provide valuable insights into the feasibility of using CP-treated plant protein as a novel green-label ingredient in plant-based formulations.

## 2. Materials and methods

### 2.1 Materials

Oat protein with ~55% protein content (PrOatein) was sourced from Lantmannen Oats, Sweden. All chemicals used in the experiments were obtained from SD Fine Chemicals Ltd, India.

### 2.2 Cold plasma treatment of oat protein

The defatting of oat protein and the cold plasma treatment were performed as described in ref. 7 without any modification. Defatted oat protein (5 g) was treated using two plasma generation voltages (170 V and 230 V) combined with two exposure times (15 min and 30 min). Samples were labeled as control

(untreated), 170-15, 170-30, 230-15, and 230-30. Plasma discharge parameters, including discharge frequency, duty cycle, and resonance frequency, remained unchanged to ensure optimized plasma glow. The sample temperature was maintained at  $28 \pm 2$  °C. Treated samples were then sealed and stored for further analysis. The schematic illustration of cold plasma system has been provided in (Fig. 1).

### 2.3 Rheometer-based intrinsic viscosity measurement of oat protein dispersion

The intrinsic viscosity of the oat protein samples was determined by a double extrapolation to zero-concentration as described in ref. 11 using the Huggins and Kraemer models provided in the eqn (1) and (2).

$$\frac{\eta_{sp}}{c} = [\eta] + K_H [\eta]^2 C \quad (1)$$

$$\frac{\ln \eta_{rel}}{c} = [\eta] + K_K [\eta]^2 C \quad (2)$$

Here  $\eta_{sp}$  is the specific viscosity (viscosity of the solvent/viscosity of the sample solution);  $\eta_{rel}$  is the relative viscosity (viscosity of the sample solution/viscosity of the solvent);  $C$  is the concentration of the sample solution;  $K_H$  is the Huggins constant and  $K_K$  is the Kramers constant.

The viscosity of the protein solutions at concentrations ranging from 0.5–2.5% (w/v) was measured using the Anton Paar rheometer by shearing with a parallel plate of 10 mm geometry. The distance between the plates was maintained at 1 mm and the temperature of the plate was kept at 25 °C. The shear rate was 0.1–100 s<sup>-1</sup> within which the shear stress exhibited by the sample solutions varied linearly with the shear rate. Within the linear flow regime, viscosity at a specific shear rate (50 s<sup>-1</sup>) was used to calculate the specific and relative viscosity of the solution. The measured values were then fitted to the Huggins (1) and Kramer models (2) using linear regression to determine the intrinsic viscosity of the protein solutions.

### 2.4 Water contact angle (WCA)

The WCA of the control and cold plasma treated oat protein was studied by the sessile drop method<sup>12</sup> without any modification. A thin layer of powdered samples was evenly spread on a glass

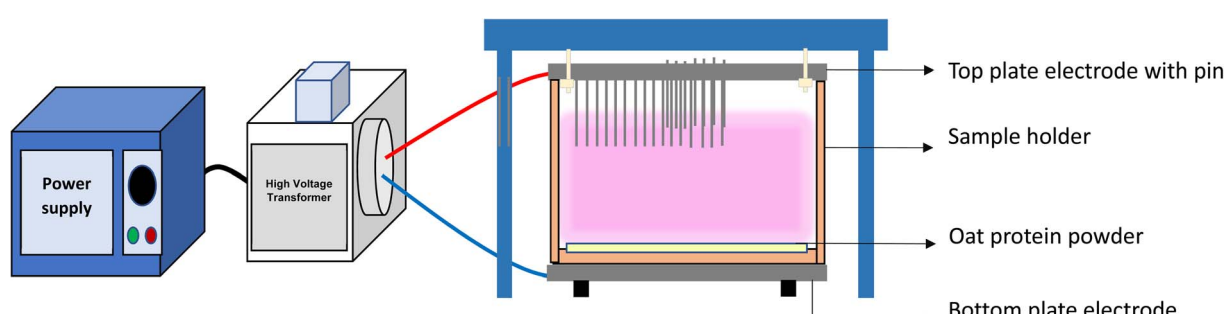


Fig. 1 Cold plasma treatment of oat protein powder.



slide. 10 images per sample were captured using a high-resolution handheld digital single-lens reflex camera after placing 10  $\mu\text{L}$  of water on the surface of the sample. Furthermore, the images were assessed for the contact angle using ImageJ software with the drop analysis-LABDSA plugin.<sup>13</sup>

## 2.5 Rheological behavior of oat protein dispersions

### 2.5.1 Steady shear flow behavior of oat protein dispersions.

The flow behavior of the control and treated oat protein dispersions was studied using an Anton Paar rheometer MCR 302 with a parallel plate of diameter 25 mm (PP/25) using the methodology given in ref. 14 with slight modification. The 20% oat protein dispersions were prepared and stored at 4 °C for overnight hydration. The oat protein dispersions were placed between the plates and the distance was adjusted to 1 mm. The samples were sheared at a rate of 1–100  $\text{s}^{-1}$  and the apparent viscosity was measured at 50  $\text{s}^{-1}$  for all the samples. The rheological behavior, based on the obtained viscosity under applied shear, was studied by fitting in the power-law model (3).

$$\sigma = K\gamma^n \quad (3)$$

where  $\sigma$  – shear stress (Pa);  $\gamma$  – shear rate ( $\text{s}^{-1}$ );  $K$  – consistency index (Pa s);  $n$  – flow behavior index.

**2.5.2 Oscillatory-frequency dependent rheological characteristics of oat protein dispersions.** The frequency-dependent rheological characteristics of untreated and cold plasma treated oat protein dispersion (20%) were studied using an Anton Paar rheometer MCR 302 with a parallel plate of diameter 25 mm (PP/25) using the method given in ref. 12. The frequency-dependent rheology was evaluated in the range of 100 Hz to 0.1 Hz at a constant strain of 0.2%. The temperature of the parallel plates was maintained at 25 °C throughout the experiment. Furthermore, the frequency-dependent behavior (the complex visco-elastic moduli against the angular frequency) was fitted with the power-law model given below,

$$G^* = K_\eta^* \omega^{n_\eta^*} \quad (4)$$

where  $G^*$  is the complex visco-elastic moduli,  $\omega$  is the angular frequency, and  $K_\eta^*$  and  $n_\eta^*$  are the model constants.

**2.5.3 Temperature-dependent rheological characteristics of oat protein dispersions.** The temperature-dependent rheological characteristics of oat protein dispersions (20%) were studied using an Anton Paar rheometer MCR 302 with a parallel plate of diameter 25 mm (PP/25). The temperature was ramped up from 25 °C to 95 °C and reduced back to 25 °C. The rate of change in temperature was kept at 5 °C  $\text{min}^{-1}$  while the gap between the plates was maintained at 1 mm. The storage ( $G'$ ) and loss modulus ( $G''$ ) were recorded to understand the temperature-dependent rheological characteristics.

## 2.6 Protein solubility

Solubility of the protein samples was determined using the biuret methodology as followed in ref. 10 with slight modification. Protein dispersions (100 mg  $\text{mL}^{-1}$ ) were prepared and

adjusted to pH 11, and then mixed for 180 min using a rock shaker. After centrifugation (8000 rpm, 30 min), the supernatants were collected. A 50  $\mu\text{L}$  aliquot of the supernatant was mixed with 200  $\mu\text{L}$  of Biuret reagent in a 96-well microplate, incubated for 40 min, and analyzed at 540 nm using a Biotek microplate reader. Absorbance values were compared to a BSA standard curve. Protein solubility (%) was calculated as the ratio of soluble protein content to total protein content determined by Kjeldahl estimation.

## 2.7 Thermal properties

**2.7.1 Differential scanning calorimetry (DSC).** The thermal properties of control and treated oat protein samples were evaluated using a TA-60WS DSC (Shimadzu Analytical Pvt. Ltd, Singapore).<sup>15</sup> 7 mg of oat protein powder was weighed and tightly sealed in a hermetic aluminum pan. The pans were heated from 30 °C to 150 °C at a heating rate of 10 °C  $\text{min}^{-1}$ . The thermal parameters such as onset temperature ( $T_o$ ), denaturation temperature ( $T_d$ ), and enthalpy ( $\Delta H$ ) were recorded.

**2.7.2 Thermal aggregation of oat protein.** A turbidimetry experiment to determine the aggregation effect of control and treated oat protein samples was conducted.<sup>4</sup> Protein dispersions of (1 mg  $\text{mL}^{-1}$ ) were prepared in a test tube and sealed to avoid evaporation. The tubes were heated for 10 min at different temperatures of 60 °C, 70 °C, 80 °C, 90 °C, 100 °C and 110 °C. After cooling the tubes, the turbidity readings were recorded in triplicate at 500 nm.

## 2.8 Impact of cold plasma on gelation properties of oat protein gels

**2.8.1 Oat protein gel preparation.** The oat protein gels were prepared from control and cold plasma-treated samples as given in ref. 16. Oat protein dispersions of 20% were prepared in glass test tubes and sealed tightly using cotton plugs. The dispersions were mixed thoroughly and kept in an ultrasonication bath for 15 seconds to remove the bubbles. Furthermore, the test tubes were heated at 110 °C for 20 min in an oil bath. After heating, the test tubes were chilled in an ice bath and stored overnight under refrigeration. The gels were carefully removed from the test tubes and used for further analysis.

**2.8.2 Rotational and oscillatory rheological characterization of protein gels.** The rheological characteristics such as steady shear flow behavior and oscillatory-frequency dependent rheology of the protein gels were evaluated using the same methodology applied to the oat protein dispersions. The amplitude sweep rheological behavior of the gels was studied using the same measuring geometry by shearing the gels from 0.01% to 100% strain (amplitude) at a constant angular frequency of 0.1 Hz. The visco-elastic moduli of the gels in the linear visco-elastic regime, within which the moduli varied linearly, were determined along with the critical strain ( $\gamma_c$  %) and loss factor ( $\tan \delta$ ) of the gels.

**2.8.3 Water holding capacity (WHC) of oat protein gels.** The water holding capacity was evaluated for gels prepared from



both the treated and control oat protein. The gel samples (0.5 g) were transferred into pre-weighed centrifuge tubes and the initial tube weight was noted; the samples were centrifuged at 6000 rpm at 25 °C for 10 min. The weight of the gels after centrifugation was measured and the WHC was measured using the following formula,

$$\text{Water holding capacity (WHC)\%} = 100 - \left\{ \frac{1 - \text{final gel weight}}{\text{gel sample weight (g)}} \right\} \quad (5)$$

**2.8.4 Texture profile of oat protein gels.** The strength and mechanical properties of oat protein gels were evaluated using a texture analyzer (Stable Microsystems TA.XTplusC). A P/5 aluminium cylindrical probe, coupled with a 50 N load cell, was used to compress the gels to 50% deformation. The test speed was set at 1 mm s<sup>-1</sup>, while the pre-test and post-test speeds were maintained at 5 mm s<sup>-1</sup>. Gel strength was measured as the peak force exerted during compression. All experiments were conducted in duplicate.

## 2.9 Application and impact of cold plasma treated oat protein on patties

The impact of cold plasma-treated oat protein in patties was evaluated by incorporating the control and treated oat protein into patties and compared with patties made without the addition of patties. 80 g of dried texturized vegetable protein was soaked in 400 mL of distilled water for 30 min, after which the excess water was squeezed out and the TVP shredded using a domestic blender. A mixture was prepared by mixing the minced TVP with the control and treated oat protein in the ratio of 1 : 10. Then 10 g round-shaped patties were made from the mixture, stored at 10 °C and used for further analysis. The patties were brought to room temperature and cooked in a pan with 5 mL of oil on both sides for 2 min until golden brown color. Furthermore, the cooked and uncooked patties were subjected to various analyses as described below.

## 2.10 Syneresis of patties

The uncooked patties were frozen at -18 °C for 48 h and then thawed at 4 °C for 1 h. After removing excess water from syneresis using tissue paper, the patties were weighed. Thawing loss (%) was determined by calculating the ratio of weight loss (g) to the initial weight of the patties.

## 2.11 Cooking loss and moisture retention of patties

The cooking loss of the patties was measured from the weight difference observed before cooking ( $P_1$ ) and after cooking using ( $P_2$ ) the following formula (6),

$$\text{Cooking loss (\%)} = \frac{(P_1 - P_2)}{A_1} \times 100 \quad (6)$$

The moisture retained by the cooked patties was evaluated by the hot air oven method (AOAC 95.46) where the patties were dried at 135 °C for 2 h.<sup>11</sup>

## 2.12 Compression juice loss in cooked patties

The compression analysis of cooked patties was carried out using a texture analyzer equipped with a P/45 aluminium probe, ensuring uniform testing. The procedure was adapted with minor modifications from ref. 17. The experiment parameters included a pre-test and post-test speed of 5 mm s<sup>-1</sup> and a test speed of 1 mm s<sup>-1</sup>, with 50% target compression and a trigger force of 5 g. The weight of the patties was measured before and after compression to assess juice loss.

## 2.13 Texture characteristics of cooked patties

The texture profile of cooked patties was evaluated using a texture analyzer equipped with a P/1 aluminium cylindrical probe. The analysis was conducted in strain mode, applying 25% strain to the patties. The pre-test, test, and post-test speeds were all set at 5 mm s<sup>-1</sup>. Textural attributes, including hardness, springiness, chewiness, and adhesiveness, were recorded using texture analyzer software.

## 2.14 Statistical analysis

All analyses were done in triplicate. The statistical significance between the samples was studied using Tukey's Honestly significant difference test at a 95% confidence interval in SPSS software (IBM SPSS Statistics version 26).

## 3. Results and discussion

### 3.1 Effect of cold plasma on the intrinsic viscosity of oat protein dispersion

The intrinsic viscosity of the oat protein dispersions with and without cold plasma treatment was analyzed and is provided in Table 1. The intrinsic viscosity of the oat protein was found to be ~1.7 dL g<sup>-1</sup> which is relatively higher than that of sodium caseinate (~1.21 dL g<sup>-1</sup>) reported in the literature.<sup>11</sup> This demonstrates the ability to use plant-sourced protein as a potential alternative to conventional animal protein. It was observed that there was a slight change in the intrinsic viscosity of plasma-treated oat protein compared to the untreated sample. Statistically, there was no significant ( $p > 0.05$ ) change in the intrinsic viscosity observed with 170-15, and 170-30 plasma treatments while 230-15 and 230-30 conditions showed a significant and sequential reduction ( $p < 0.05$ ) in intrinsic viscosity compared to the untreated oat protein. The lowest intrinsic viscosity was observed for the 230-30 oat protein which was 4% less than that of the untreated oat protein. Intrinsic viscosity of a biopolymer depends on the hydrodynamic volume of the polymer, which is influenced by its molecular weight/chain length and hydrophilic interaction.<sup>18</sup> The larger the hydrophilic interaction, the larger the hydrodynamic volume and thus the higher the intrinsic viscosity. The decreased intrinsic viscosity observed in plasma-treated oat protein dispersions indicates a reduction in the hydrodynamic volume due to increased



Table 1 Intrinsic viscosity ( $\eta$ ), Huggins ( $K_H$ ) and Kraemer ( $K_K$ ) constants obtained for oat protein solutions<sup>a</sup>

Protein in solution	$\eta$ (dL g <sup>-1</sup> )	$K_H$	$K_K$
Control	1.794 ± 0.030 <sup>a,1</sup>	-0.212 ± 0.002 <sup>a,1</sup>	-0.965 ± 0.072 <sup>a,1</sup>
170-15	1.797 ± 0.009 <sup>a,1</sup>	-0.212 ± 0.001 <sup>a,1</sup>	-0.946 ± 0.022 <sup>a,1</sup>
170-30	1.781 ± 0.008 <sup>a,1</sup>	-0.214 ± 0.000 <sup>a,1</sup>	-0.888 ± 0.023 <sup>a,1</sup>
230-15	1.761 ± 0.018 <sup>b,1</sup>	-0.217 ± 0.002 <sup>b,2</sup>	-0.812 ± 0.126 <sup>a,1</sup>
230-30	1.715 ± 0.043 <sup>b,1</sup>	-0.218 ± 0.003 <sup>b,2</sup>	-0.917 ± 0.019 <sup>a,1</sup>

<sup>a</sup> The values having different alphabets in the superscripts are statistically significant corresponding to voltage while the values having different numerical alphabets are statistically significant corresponding to the treatment time.

hydrophobicity. The author's previous study on the characterization of plasma-treated oat protein revealed an increase in the hydrophobicity of the oat protein<sup>10</sup> after plasma treatment which corresponds to the present observation. Surface hydrophobicity has an inverse relationship with intrinsic viscosity as the hydrodynamic volume is reduced with reduced hydration. Irrespective of the aggregation phenomenon observed in oat protein after cold plasma treatment, the intrinsic viscosity is primarily influenced by the hydrophilic interactions of the protein. To support this, the water contact angle of the oat protein, an indication of surface hydrophobicity, also showed an increase after cold plasma treatment. The constants obtained from the Huggins and Kramers models ( $K_H$  and  $K_K$ ) are also provided in Table 1 to understand the solvation properties of the protein. Both the model constants were observed to be negative for all oat protein samples, regardless of the cold plasma treatment. As quoted in the literature, negative  $K_H$  and  $K_K$  values indicate an amphiphilic attribute of the protein.<sup>19</sup> Due to this amphiphilic nature, the plant proteins tend to form heterogeneous dispersions with water. Also,  $K_K$  values ranging from 0.5–1 correspond to the inherently poor solvation characteristics of the oat protein.<sup>20</sup> Despite the observed deviations, intrinsic viscosity does not depict the effect of cold plasma treatment on the oat protein as the inherent hydrophobicity of protein predominantly influences the intrinsic viscosity.

### 3.2 Water contact angle

The water contact angle (WCA) measurements are instrumental in assessing the wettability and surface energy of biomolecules.

These measurements provide insights into how plant proteins interact with water, which is crucial for applications in food science, biomaterials, and surface modification technologies. The effect of cold plasma on the water contact angle of oat protein is depicted in Fig. 2. The water contact angle value increased for all the plasma-treated samples. The highest water contact angle value (104.06 ± 5.81°) was observed for the 230-30 sample while the lowest water contact angle (93.64 ± 3.14°) was observed for the control sample. As the plasma-generated free radicals react with the oat protein, non-polar amino acids are released via surface etching and peptide bond cleavage. This, in turn, increases the temporary hydrophobic behavior and reduces wettability.<sup>21</sup> The WCA result is highly dependent on the balance between polar and non-polar amino acids and the surface energy of the protein molecules.<sup>22</sup> The input parameters such as voltage and exposure time affected the WCA result; lower exposure times tend to increase the wettability. Similarly, at an exposure time of 15 min, an increase in voltage reduced the wettability, as indicated by a lower WCA. However, prolonged exposure times increased the WCA, indicating the hydrophobic nature of the protein surface. The particle size reduction under higher treatment conditions also results in increased hydrophobicity due to the exposure of non-polar amino acids and re-aggregation of protein particles.<sup>23,24</sup> Thus, by controlling the input parameter the functionality of proteins can be tailored for various food applications.

### 3.3 Effect of cold plasma on rheological properties of oat protein dispersion

**3.3.1 Steady shear rotatory rheology.** The steady shear rheology of the oat protein dispersions is given in Fig. 3. The viscosity of the dispersions sequentially reduced with the increase in the shear rate in all dispersions regardless of the cold plasma treatment. This is due to the shear-thinning nature of hydrated oat protein particles, which tend to align with the direction of shear forces. The viscosity of the cold plasma-treated dispersions was observed to be higher than that of the control oat protein dispersion. The highest viscosity was exhibited by the 170-15 sample followed by 170-30, 230-15, and 230-30 samples. The shear stress and the shear rate were fitted with the power law model to obtain the model constants, *i.e.*, the flow index and consistency index which are provided in Table 2 along with the apparent viscosity at 50 s<sup>-1</sup>. The power law model exhibited an excellent fit with the  $R^2$  values in the

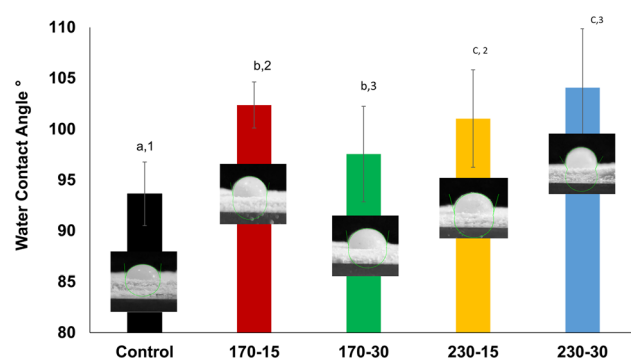


Fig. 2 Effect of cold plasma on the water contact angle of oat protein powders.



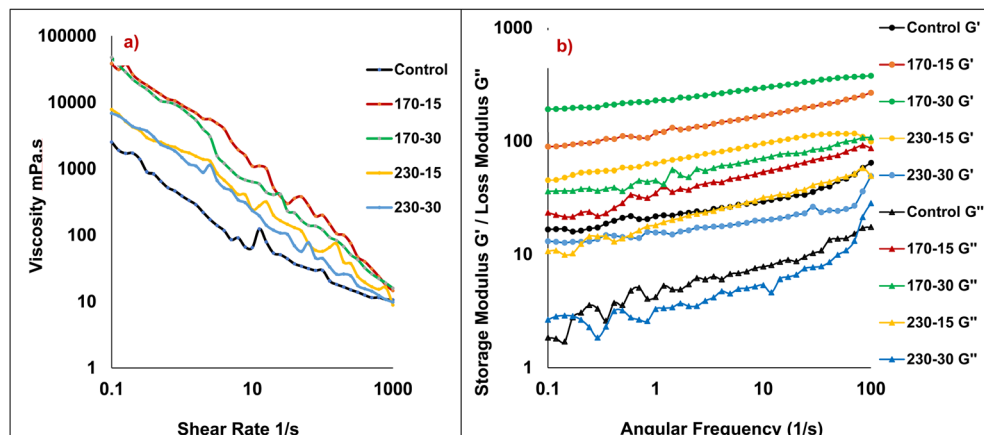


Fig. 3 Effect of cold plasma on (a) steady shear and (b) oscillatory – frequency dependent rheological characteristics of oat protein dispersions.

Table 2 Effect of cold plasma on rheological constants of 20% oat protein dispersion<sup>a</sup>

Sample	Shear dependent constants			Apparent viscosity @ 50 s <sup>-1</sup>	Relative protein solubility% at 11 pH	Frequency dependent constants		
	$K_\eta$	$n_\eta$	$R_\eta^2$			$K_\eta^* (\times 10^5)$ (Pa)	$n_\eta^*$	$R_\eta^{*2}$
Control	405.15	0.981	0.950	$34.03 \pm 1.41^{a,1}$	$0.04 \pm 0.02^{a,1}$	0.222	-0.821	0.996
170-15	8197.50	0.821	0.988	$380.31 \pm 0.89^{b,1}$	$0.05 \pm 0.01^{a,1}$	2.100	-0.830	0.999
170-30	4525.25	0.871	0.982	$166.79 \pm 1.25^{b,1}$	$0.09 \pm 0.04^{a,2}$	3.374	-0.888	0.997
230-15	1657.33	0.532	0.967	$115.37 \pm 1.04^{ab,1}$	$0.04 \pm 0.01^{a,1}$	0.303	-0.852	0.977
230-30	1408.72	0.692	0.988	$56.83 \pm 0.26^{ab,1}$	$0.11 \pm 0.01^{a,2}$	0.237	-0.786	0.947

<sup>a</sup> The values having different alphabets in the superscripts are statistically significant corresponding to voltage while the values having different numerical alphabets are statistically significant corresponding to the treatment time.

range of 0.950–0.988. The consistency index and apparent viscosity of the oat protein dispersions also followed the same pattern, with the highest values observed for the 170-15 sample followed by 170-30, 230-15, 230-30, and the control. These observations are consistent with the findings of our structural investigations of oat protein after cold plasma treatment<sup>10</sup> wherein the low-intensity plasma treatment (170-15) induced aggregation of the proteins and increased the particle size. Nonetheless, as the treatment intensity increases with the rise in voltage and treatment time the polymeric chains and aggregates are cleaved to a reduced size. This is majorly attributed to the observed pattern of changes in the apparent viscosity and consistency index. Despite the observed viscosity reduction on shearing, the flow index value is ~0.981 for the control oat dispersion showing its near-Newtonian fluid behavior. This is due to the less hydrophobic nature of the control oat protein which facilitates better hydration and affinity with the water molecules compared to the plasma-treated ones. The observed increase in the water contact angle of the plasma-treated oat protein also substantiates the increased hydrophobicity and thus the reduced hydration. This resulted in the amplified pseudo-plastic behavior, as demonstrated by the reduced ' $n$ ' values in the plasma-treated oat protein dispersions.

**3.3.2 Frequency-dependent oscillatory rheology.** The frequency-dependent oscillatory rheological properties of the

oat protein dispersion were studied and the changes in the visco-elastic moduli are presented in Fig. 3b. All the oat dispersions exhibited an increase in both the storage ( $G'$ ) and loss ( $G''$ ) moduli with increasing oscillating frequency. As the oscillating shear entangles the protein polymeric chain structure, the resistance offered to the flow would increase which leads to a rise in the visco-elastic moduli of the dispersions. Nevertheless, the slopes of the moduli exhibited by the control and 230-30 samples are observed to be more significant than those of the other samples indicating a large dependency on the oscillating frequency.<sup>25</sup> This demonstrates that the protein conformational structure notably influences its rheological dependency. Since cold plasma treatment induces oat protein aggregation, 170-15, 170-30, and 230-15 samples showed increased aggregate sizes compared to the control and 230-30 samples. The smaller the size of the protein particles, the greater the frequency dependency observed showing a weak gel nature.

In addition, the storage modulus ( $G'$ ) was greater than the loss modulus ( $G''$ ) value for all oat protein dispersions showing a more elastic than viscous behavior. The predominant storage moduli indicate an elastic weak gel nature associated with ordered protein chain regions.<sup>26</sup> Also, no cross-over of  $G'$  and  $G''$  over the oscillating frequency range was observed, indicating the absence of gel-to-sol transition or the breakdown of



the elastic gel structure. These rheological characteristics remained unchanged even after the plasma treatment; however the moduli were observed with a notable increase. Among all the plasma-treated samples, 170-30 displayed higher  $G'$  and  $G''$  values followed by 170-15, 230-15, and 230-30. The control, *i.e.* untreated oat dispersions were observed with the smallest visco-elastic moduli. This is again an attribute of aggregated protein particles induced by cold plasma which are of larger size and show an increased modulus. As the intensity of plasma treatment increases, the protein aggregates deform and disintegrate into smaller fragments, demonstrating rheological characteristics equivalent to the untreated oat dispersion.

**3.3.3 Temperature dependent rheology.** The visco-elastic moduli of the oat dispersions over thermal gelation were studied to understand the sol–gel transition and are represented in Fig. 4. Both the storage and loss modulus values decrease on heating and further increase sequentially on cooling depicting the process of thermal gelation. The process of conversion of heterogeneous oat dispersion into a structural gel network through a sequence of reactions is known as protein thermal gelation. The addition of thermal energy on heating provides kinetic energy to the molecules and initiates protein unfolding. This causes the molecules to adopt a linear state, allowing them to glide along the shear force thus exhibiting reduced visco-elastic moduli. Furthermore, the unfolding process exposes the buried hydrophobic structures on the surface and initiates hydrophobic interactions among the subunits. This protein–protein interaction propagates further to form aggregates and structural networks on cooling, resulting in increased visco-elastic moduli. There was a remarkable difference between the initial (before heating) and final (after cooling) storage and loss modulus values of the respective samples. The final modulus values were found to be more than the initial values which indicates the progression of gelation. Additionally, the increased hydration might facilitate swelling

of the molecules, thus synergistically raising the hydrodynamic volume along with protein–protein aggregation. This would also contribute to higher visco-elastic moduli.

It was surprising to observe that all the plasma-treated oat dispersions, except 230-15, exhibited a reduced visco-elastic modulus compared to the untreated one while the 230-15 sample and the untreated oat protein showed comparable values. This observation is quite contradictory to the rheology of the dispersions which indicates the significant influence of thermal energy in inducing aggregation and network formation. The cold plasma treatment has been reported to cause peptide cleavage followed by the formation of large and small aggregates through protein unfolding and alterations in the surface charge potential. The authors in their previous study<sup>10</sup> confirmed that at low intense plasma exposure (170-15 and 230-15), the aggregates are larger while at high intense exposure (170-30 and 230-30), the particle size is reduced. Additionally, the  $\zeta$ -potential was observed to be reduced with the increase in intensity of cold plasma treatment. Even though both 170-15 and 230-15 have an increased particle size due to unfolding and aggregation, the 230-15 sample possesses a relatively lower zeta potential compared to all the plasma-treated samples. The lower the zeta potential, the weaker the electrostatic repulsion, resulting in better networking during thermal gelation. Along with the increased particle size, the reduced zeta potential also synergistically contributes to the higher visco-elastic moduli of the 230-15 sample on thermal gelation. This proves that the surface charge of the protein plays a pivotal role in propagating the hydrophobic interactions among the proteins leading to linear and random network aggregation during gelation.

#### 3.4 Protein solubility

The effect of cold plasma on the protein solubility at pH 11 is represented in Table 2. The oat protein fractions isolated using column chromatography were reported to have notable solubility under alkaline pH conditions.<sup>27</sup> However, surprisingly, the

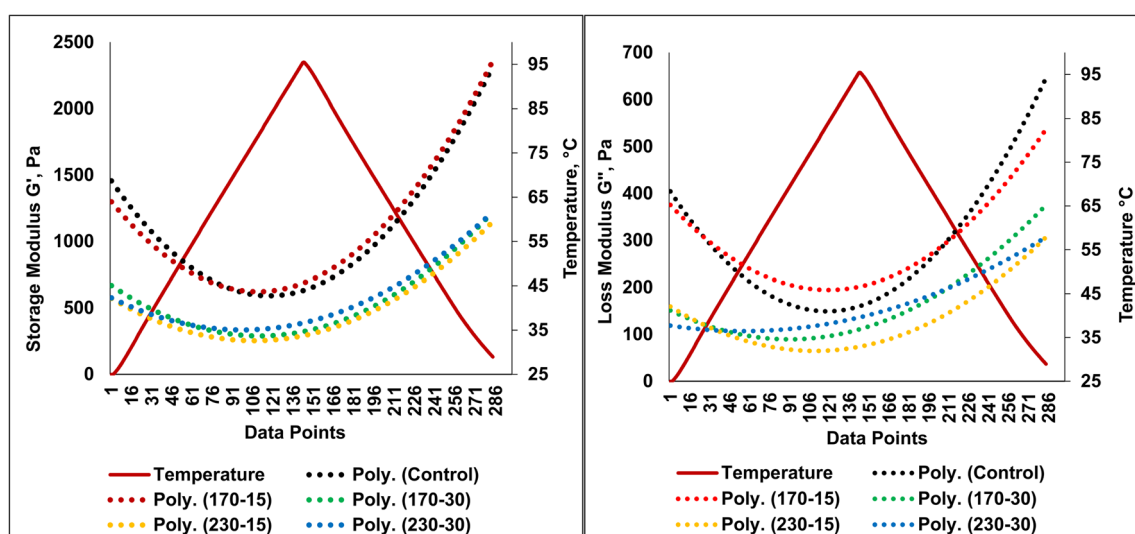


Fig. 4 Temperature dependent rheological characteristics of oat protein dispersions.



oat protein used in the present study showed low levels of solubility even under highly alkaline conditions. This might be attributed to the protein structural changes that occurred during the extraction and purification processes.<sup>28</sup> The results show that a longer treatment time leads to a slight increase in protein solubility at both the input voltages (170 V and 230 V). In general, the oat protein exhibits poor solubility due to the presence of globulins. The 15-minute treatment of protein caused fewer changes in solubility, which might be due to the effect of exposure of hydrophobic groups and milder aggregation in the proteins.<sup>26</sup> However, at longer treatment times, the plasma-induced radical reaction causes partial unfolding and size reduction in the proteins *via* surface etching and peptide cleavage, thereby resulting in an increase in the solubility of the protein.<sup>29</sup> The protein properties are highly influenced by changes in surface energy and the ratio of hydrophilic and hydrophobic amino-acid groups.<sup>24</sup>

### 3.5 Effect of cold plasma on thermal properties of oat protein

**3.5.1 Differential scanning calorimetry.** Thermal properties such as thermal denaturation play a crucial role in protein gelation. The DSC results of oat protein are provided in Table 3. It is observed from the table that the cold plasma-treated sample showed an increased onset temperature  $T_o$  °C. This

shows a delay in initiation of the reaction in the protein as compared to the control sample (65.82 °C). This might be due to cold plasma generated radical species inducing the formation of partial or disrupted protein aggregates, which in turn require higher heat energy. Similarly, the peak temperature ( $T_p$  °C) and the enthalpy of denaturation required for the protein also depend on the protein's nature and its properties. The cold plasma is capable of inducing multiple reactions on the surface of proteins through oxidation and radical reaction (ROS and RNS), thus leading to partial denaturation and oxidation in the protein molecules.<sup>30</sup> The increase in  $T_p$  °C in 170-15 and 170-30 samples indicated the formation of protein aggregates after plasma treatment. However, an increase in input voltage from 170 V to 230 V, while keeping the exposure time constant, resulted in a reduced denaturation temperature  $T_p$  (93.29 °C), possibly due to the aggregate disruption resulting in a reduction in the thermal stability of protein. This is in line with our previous studies on particle size measurement.<sup>10</sup> In the case of 30 min treatments, the increase in voltage caused an increase in denaturation temperature as compact and firm aggregates were formed due to the high-intensity treatment, resulting in an increased temperature requirement for denaturation. Similarly, the reduced enthalpy ( $\Delta H$ ) requirement in the 30 min treatment indicates exposure of the hydrophobic core and formation of smaller aggregates, consistent with the results in ref. 16 and 31. Thus, the plasma treatment condition of 230-15 demonstrates a balanced approach for achieving the desired protein functionality, which would result in a decreased temperature requirement for protein gelation.

**3.5.2 Thermal aggregation.** The impact of varying temperature on the aggregation properties of the control and the cold plasma-treated samples is shown in Fig. 5. Turbidity refers to the resistance to light transmission through the aliquot, indicating the properties such as size and nature of the particles in the dispersion. The treated sample showed relatively reduced absorbance at 500 nm indicating the reduction in turbidity

Table 3 Effect of cold plasma on DSC of 20% oat protein dispersions

Sample	$T_o$ , °C	$T_p$ , °C	$T_{end}$ , °C	Enthalpy ( $\Delta H$ ) (J g <sup>-1</sup> )
Control	65.82	100.18	120.31	76.48
170-15	75.96	115.36	134.68	91.42
170-30	121.34	124.46	128.34	4.1
230-15	66.86	93.29	114.8	71.44
230-30	128.67	131.11	134.49	0.57

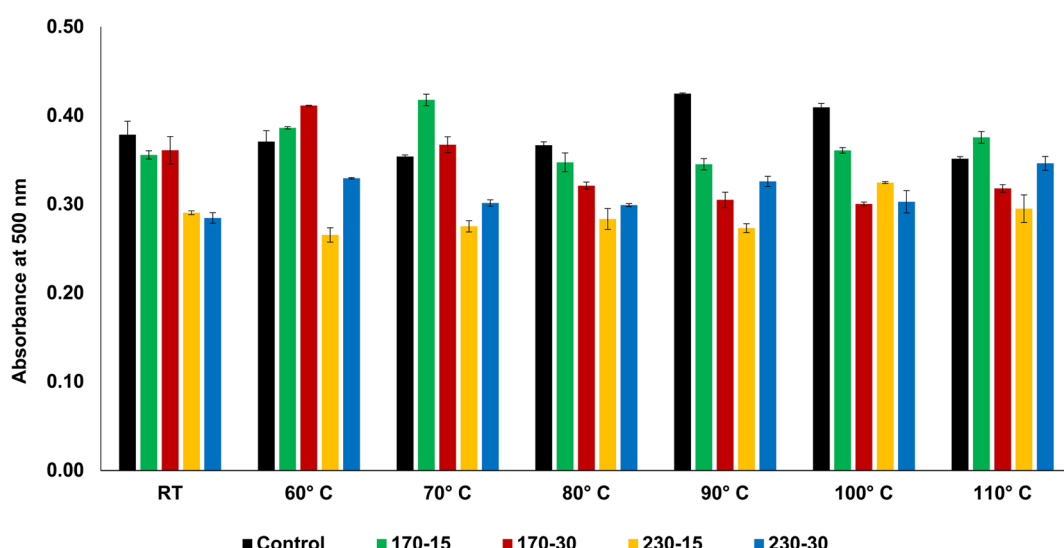


Fig. 5 Effect of cold plasma on thermal aggregation of oat protein at different temperatures.

irrespective of the heating temperature. The 230-15 sample exhibited the lowest turbidity among the treated samples. The turbidity reduction is directly related to the protein aggregates induced by the heating process among the plasma-treated samples. Although the aggregation of macromolecules is said to increase the turbidity and absorbance, the surface energy of the protein molecule resulting from the plasma treatment might have influenced the increase in aggregation thereby transmitting more light through the protein dispersion. In response to the change in heating temperature, the increase in temperature showed a decrease in absorbance in the control sample. A similar observation was found in the treated samples up to 100 °C, however, with a further increase to 110 °C an increase in absorbance was observed. This might be due to the

partial unfolding and loosening of protein aggregates at higher temperatures supporting better dispersions at higher temperatures, suitable for thermally processed protein drinks.

### 3.6 Impact of cold plasma on gelation properties of oat protein gels

Oat protein gels were prepared using a heating method, resulting in soft gels. To evaluate the effect of cold plasma on the gelation properties of modified oat protein, the sample was heated at 110 °C for 20 min in an oil bath. The prepared gels were then analysed for rheological properties, and their water-holding capacity was measured as described below.

**3.6.1 Steady shear rheology of the oat protein gels.** The prepared gels from control and plasma-treated oat protein

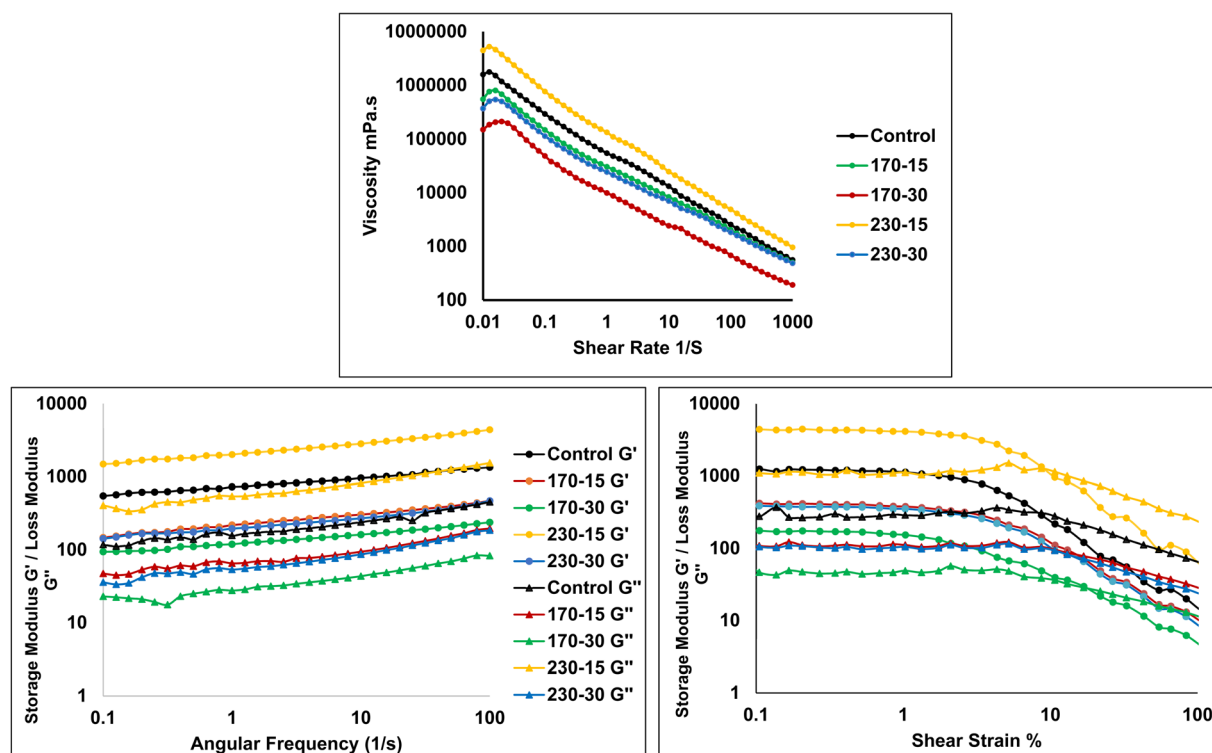


Fig. 6 Effect of cold plasma on (a) steady shear; (b) oscillatory – frequency dependent and (c) amplitude dependent rheological characteristics of oat protein gels.

Table 4 Effect of cold plasma on rheological constants and water holding capacity of oat protein gels<sup>a</sup>

Samples	Shear dependent constants			Apparent viscosity at 50 s <sup>-1</sup>	WHC (%)	Frequency dependent constants		
	$K_\eta$ ( $\times 10^5$ ) (Pa)	$n_\eta$	$R_\eta$ <sup>2</sup>			$K_\eta^*$ ( $\times 10^5$ ) (Pa)	$n_\eta^*$	$R_\eta$ <sup>2</sup>
Control	0.627	-0.698	0.998	$4149.95 \pm 605.15^{\text{a,1}}$	$99.00 \pm 0.08^{\text{a,1}}$	7.721	-0.889	0.997
170-15	0.362	-0.635	0.994	$3212.55 \pm 257.85^{\text{b,2}}$	$91.07 \pm 0.86^{\text{b,2}}$	2.353	-0.861	0.999
170-30	0.116	-0.648	0.991	$1994.33 \pm 25.38^{\text{b,3}}$	$75.91 \pm 0.25^{\text{b,3}}$	1.318	-0.871	0.998
230-15	1.476	-0.749	0.997	$7981.75 \pm 26.35^{\text{c,2}}$	$99.41 \pm 0.16^{\text{c,2}}$	2.500	-0.870	0.999
230-30	0.289	-0.611	0.994	$2698.05 \pm 142.75^{\text{c,3}}$	$77.84 \pm 0.78^{\text{c,3}}$	2.160	-0.865	0.999

<sup>a</sup> The values having different alphabets in the superscripts are statistically significant corresponding to voltage while the values having different numerical alphabets are statistically significant corresponding to the treatment time.



dispersions were subjected to a steady shear rate and the viscosity is presented in Fig. 6a. The protein gels exhibited a reduced viscosity with continuous shearing. With initial shearing, the viscosity rises at low shear rates followed by a sequential reduction upon further shearing. The gels made from 230-15-treated oat protein showed the highest viscosity followed by the control, 170-15, and 230-30. 170-30 treated oat protein gels have the lowest viscosity. The shear stress and the shear rate were fitted with the power law model to obtain the model constants *i.e.* flow index and consistency index which are provided in Table 4 along with the apparent viscosity at 50 s<sup>-1</sup>. The power law model exhibits an excellent fit with the  $R^2$  value greater than ~0.99. The consistency index and the apparent viscosity of the oat protein dispersions also followed the same pattern with 230-15 showing the highest values followed by the control, 170-15, 230-30, and 170-30. These findings are contradictory to those observed in their corresponding dispersions which might be attributed to the hydration and thermo-gelation process. On heating, the thermal denaturation of the proteins results in protein aggregates holding water molecules trapped in a three-dimensional network. This remarkably alters the nature of the protein dispersion compared to the gels formed thereafter. Nevertheless, the observed trend in the viscosity of plasma-treated gels would be the result of stable and stronger aggregate production with 230-15 plasma treatment leading to the highest viscosity (~7981.75 cP). Although the 170-15 treatment also facilitated aggregate formation, the thermal stability might play a role in maintaining the strength resulting in a similar viscosity to that of the control (~3212.55 cP). Additionally, 170-15 treated oat protein with larger aggregates might prevent the disassociation of protein on heating and thus inhibit the formation of a gel network.<sup>32</sup> The gels made from proteins exposed to longer duration (170-30; 230-30) had lower viscosity (1994.33 cP; 2698.05 cP) and consistency index as a result of distorted smaller protein aggregates. Smaller and weaker aggregates exhibited less resistance on shearing resulting in reduced viscosity and consistency index of the gels.

**3.6.2 Frequency-dependent behavior of the oat protein gels.** The oscillatory rheology of the oat protein gels with varying frequencies is given in Fig. 6b. The storage and loss moduli of the gels continuously vary with the increase in oscillatory shearing frequency showing a strong frequency-dependent behaviour. The storage moduli ( $G'$ ) are greater than the loss moduli ( $G''$ ) in all the samples owing to the elastic nature of the gels. The oat protein gels remained stable as the oscillating frequency increased, with the moduli never crossing over. The complex moduli of the gels against the oscillating frequency were fitted to the power law model and the model constants are given in Table 4. The model presented an excellent fit with  $R^2$  values > 0.99 in all the gels while the  $n_{\eta}^*$  values were >~0.88 demonstrating a strong frequency-dependent behaviour. Nevertheless, in all the protein gels, as the angular frequency increases, the moduli also rise, possibly due to the alignment of aggregates caused by the frequent oscillating shear.<sup>33</sup> Among all the gels, the 230-15 treated protein gels displayed the highest moduli followed by the control sample. The 170-30 treated oat protein gel exhibited the lowest moduli, whereas the 170-15 and

230-30 treated gels displayed similar oscillatory rheological behaviour. These findings contrast sharply with the oscillatory rheological properties of their dispersions, particularly the 170-30 treated oat protein dispersion, which demonstrated the highest moduli with increasing oscillating frequency. This might be due to the aggregated structure's resistance to unfolding and re-association on heating. Similarly, the intensely treated protein (230-30) having the smallest aggregates and highest zeta potential demonstrated electrostatic repulsion which prevents protein–protein interaction on heating. This would have caused the weaker gel structure and thus the lower moduli. The positive zeta potential and the relatively larger aggregates of 230-15 samples facilitated the formation of gels with stronger visco-elastic moduli. Thus, the plasma-treated proteins at the highest voltage and shorter duration would be desirable for applications requiring stronger gel networks *e.g.* to develop plant protein-based meat analogues.<sup>34</sup>

**3.6.3 Amplitude-dependent behavior of the oat protein gels.** The visco-elastic moduli of the oat protein gels with increasing amplitude or strain are provided in Fig. 6c. It was observed that the visco-elastic moduli tend to decrease beyond the linear visco-elastic regime (<~1.33% shear strain) corresponding to the increase in the amplitude. The untreated as well as plasma treated protein samples exhibited similar linear visco-elastic regimes beyond which inclined to reduce sequentially for a gel–sol transition. At lower shear strains, the elastic moduli ( $G'$ ) of the protein gels were higher than the viscous moduli ( $G''$ ). As the shear strain increases, the elastic moduli decrease sequentially while the viscous moduli increase. At specific strain values, the moduli crossed over and the viscous moduli predominated beyond this point owing to the transition of the gel network to a viscous flowing sol. The linear visco-elastic moduli were higher for the 230-15 treated plasma protein gels followed by the control sample, 170-15, 230-30, and 170-30. Remarkable differences were seen in the elastic moduli *i.e.* the highest  $G'$  (3682.40 Pa) was shown by 230-15 samples while the lowest  $G'$  (131.55 Pa) was observed in 170-30 samples. It was anticipated that the plasma-induced aggregation of the protein samples would enhance the gel strength yielding higher visco-elastic moduli. However, this was true only for the 230-15 samples wherein medium-sized aggregates were formed. With larger (170-15) and smaller aggregates (170-30; 230-30) thermogelation was not facilitated as the samples exhibited inhibition of unfolding and re-structuring. This might be due to the increased negative zeta potential under these treatment conditions induced by energetic plasma reactive species and free radicals which would generate an ionic environment.

Additionally, the critical strain (%), defined as the strain beyond which the linear visco-elastic regime changes, demonstrates the stability of the gel network. The higher the critical strain of the gel, the more stable it is.<sup>35</sup> Akin to the moduli, 230-15 samples exhibited the highest critical strain (~2.11%), demonstrating their greater stability (as seen in Table 5). Despite having the second-highest moduli, the control samples showed a relatively lower critical strain (~1.39%) while all the plasma-treated samples exhibited a higher critical strain (~1.74–1.93%). The protein aggregate structure in the gel



Table 5 Effect of cold plasma on amplitude dependent parameters of oat protein gels

Sample	Critical strain, $\gamma_c$	Storage modulus, $G'_LVE$	Loss modulus, $G''_{LVE}$	Loss factor, $\tan \delta$
Control	1.39 $\pm$ 0.36 <sup>a,1</sup>	1075.5 $\pm$ 140.41 <sup>a,1</sup>	305.39 $\pm$ 42.27 <sup>a,1</sup>	0.284 $\pm$ 0.00 <sup>a,1</sup>
170-15	1.74 $\pm$ 0.00 <sup>b,2</sup>	348.34 $\pm$ 42.26 <sup>b,2</sup>	108.18 $\pm$ 0.95 <sup>b,2</sup>	0.316 $\pm$ 0.04 <sup>b,2</sup>
170-30	1.93 $\pm$ 0.19 <sup>b,2</sup>	131.55 $\pm$ 97.13 <sup>b,3</sup>	49.25 $\pm$ 36.10 <sup>b,3</sup>	0.378 $\pm$ 0.01 <sup>b,3</sup>
230-15	2.11 $\pm$ 0.00 <sup>b,2</sup>	3682.40 $\pm$ 238.00 <sup>c,2</sup>	1170.50 $\pm$ 84.50 <sup>c,2</sup>	0.318 $\pm$ 0.00 <sup>b,2</sup>
230-30	1.93 $\pm$ 0.19 <sup>b,2</sup>	310.30 $\pm$ 26.09 <sup>c,3</sup>	108.03 $\pm$ 9.36 <sup>c,3</sup>	0.347 $\pm$ 0.00 <sup>b,3</sup>

network establishes flexibility to deformation against the oscillating strain<sup>36</sup> which in turn yields higher critical strain values in the gels made from plasma-treated samples. This validates that the plasma-treated oat proteins could facilitate the formation of stable gels irrespective of their strength.

**3.6.4 Water holding capacity of oat protein gels.** The water holding capacity (WHC) is one of the important characteristics of protein gels where the desirability increases with the increase in water holding capacity. The WHC% of the control and plasma-treated OP gels are provided in Table 4. It is observed that the control (99%) and 230-15 samples (99.41%) showed a higher WHC as compared to the other samples. The application of both the input voltage (170 V, 230 V) and plasma exposure time (15 min, 30 min) has impacted the WHC of gels significantly ( $p > 0.05$ ). The milder plasma treatment tends to cause the partial aggregation of protein leading to an increase in agglomeration and particle size. This is due to the increased surface charge of protein through radical interaction.<sup>37</sup> In addition to this the plasma-induced reaction also causes the disruption of the protein core and the release of the hydrophobic group to the surface. This causes protein–protein interaction and aggregation. Thus, the loss of hydrophilic groups on the surface reduced interaction with water molecules, thereby reducing the WHC at 170 V. However, an increase in input voltage to 230 V causes different effects on the protein and WHC. Primarily at 230-15, the radicals caused the oxidative reaction, and the partial disruption of aggregates increased the hydrophilic groups thereby resulting in the highest WHC%.<sup>38</sup> The highest treatment causes protein denaturation and aggregate disruption; however, intense plasma radical exposure tends to promote the development of stronger hydrophobic aggregates, reducing the WHC% in the 230-30 samples.<sup>39</sup> Similar results of increased WHC were also observed in cold plasma treatment of peanut protein,<sup>40</sup> and pea protein.<sup>14,31</sup>

Furthermore, the desired level of WHC and gel strength could be achieved through the optimization of plasma treatment conditions.

**3.6.5 Texture profile of oat protein gels.** The texture profile analysis results of oat protein gels are provided in Table 6. The sample 230-15 showed higher values in terms of hardness, adhesiveness, cohesiveness, gumminess, and chewiness. At both 170 V and 230 V, the increase in plasma exposure time from 15 min to 30 min resulted in a decrease in texture parameters including the hardness and gumminess. This might be due to partial protein denaturation and formation of loose plasma-induced unfolded protein aggregates caused by plasma radical interaction and intermolecular hydrophobic interaction.<sup>41</sup> Similar results were observed in ref. 42, where the protein aggregates were induced by the hydrophobic interaction and disulfide bonding influencing the hardness and other texture properties. In addition to this, the increase in surface energy and surface hydrophobicity reduces the affinity for water, hence affecting the gel structure; corresponding results were evident from the result of WHC%.<sup>43</sup> The increase in voltage at 15 min and 30 min exposure time caused a significant increase in hardness and other texture parameters indicating the increased gel strength. With the increase in intensity of the treatment, the dense radical species cause the partial disruption of aggregates. The smaller size of the protein aggregates and increased hydrophobicity (stronger hydrophobic interaction) would have contributed to the formation of harder gels compared to the lower voltage treated samples. Comparatively, the 230-15 sample resulted in better textural properties such as higher hardness ( $188.96 \pm 1.21$  g) and gumminess ( $126.49 \pm 1.45$  g) and also excelled with better water holding capacity ( $99.41 \pm 0.16\%$ ). Thus, the 230-15 sample was further incorporated in the patties prepared from texturized vegetable protein and

Table 6 Effect of cold plasma on texture analysis of oat protein gels<sup>a</sup>

Sample	Hardness	Adhesiveness	Springiness	Cohesiveness	Gumminess	Chewiness	Resilience
Control	144.75 $\pm$ 2.67 <sup>a,1</sup>	26.30 $\pm$ 2.13 <sup>a,1</sup>	0.92 $\pm$ 0.01 <sup>a,1</sup>	0.62 $\pm$ 0.02 <sup>a,1</sup>	90.38 $\pm$ 2.10 <sup>a,1</sup>	83.05 $\pm$ 2.10 <sup>a,1</sup>	0.07 $\pm$ 0.01 <sup>a,1</sup>
170-15	129.75 $\pm$ 5.04 <sup>a,2</sup>	29.04 $\pm$ 0.88 <sup>a,1</sup>	0.90 $\pm$ 0.00 <sup>b,2</sup>	0.63 $\pm$ 0.04 <sup>a,1</sup>	82.44 $\pm$ 8.03 <sup>b,2</sup>	73.86 $\pm$ 6.84 <sup>b,2</sup>	0.07 $\pm$ 0.01 <sup>a,b,2</sup>
170-30	93.20 $\pm$ 5.89 <sup>b,2</sup>	23.01 $\pm$ 1.09 <sup>a,1</sup>	0.88 $\pm$ 0.00 <sup>b,2</sup>	0.63 $\pm$ 0.04 <sup>a,1</sup>	58.70 $\pm$ 7.80 <sup>b,1</sup>	51.91 $\pm$ 7.04 <sup>b,1</sup>	0.06 $\pm$ 0.01 <sup>a,b,2</sup>
230-15	120.89 $\pm$ 1.28 <sup>a,2</sup>	25.13 $\pm$ 3.00 <sup>a,1</sup>	0.89 $\pm$ 0.02 <sup>ab,2</sup>	0.59 $\pm$ 0.03 <sup>a,1</sup>	71.71 $\pm$ 4.87 <sup>c,2</sup>	64.09 $\pm$ 5.43 <sup>a,2</sup>	0.06 $\pm$ 0.00 <sup>b,2</sup>
230-30	188.96 $\pm$ 1.21 <sup>c,1</sup>	32.10 $\pm$ 0.70 <sup>a,1</sup>	0.91 $\pm$ 0.02 <sup>ab,2</sup>	0.67 $\pm$ 0.01 <sup>a,1</sup>	126.49 $\pm$ 1.45 <sup>c,1</sup>	117.31 $\pm$ 1.71 <sup>a,1</sup>	0.06 $\pm$ 0.00 <sup>b,2</sup>

<sup>a</sup> The values having different alphabets in the superscripts are statistically significant corresponding to voltage while the values having different numerical alphabets are statistically significant corresponding to the treatment time.



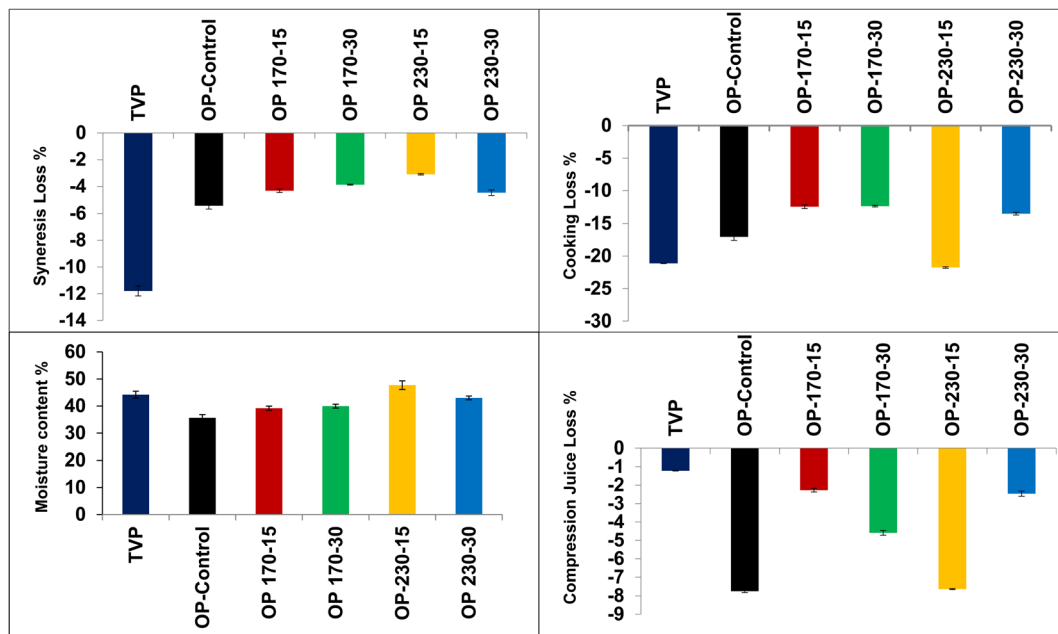


Fig. 7 Effect of cold plasma on physical attributes of patties incorporated with oat protein.

evaluated for relevant parameters such as syneresis, cooking loss, compression juice loss, and textural properties analysis.

### 3.7 Application and impact of cold plasma treated oat protein on patties

**3.7.1 Syneresis loss of patties.** The syneresis loss% of the patties prepared with and without the oat protein (control and plasma treated) is provided in Fig. 7. The addition of oat protein in the patties made from texturized vegetable protein (TVP) reduced the syneresis loss of the patties significantly. This was supported by the high water absorption and holding capacity of oat protein.<sup>10</sup> Among the oat protein-incorporated patties also, the impact of the cold plasma-treated oat protein addition further reduced the water loss and reinforced improved freeze-thaw stability. The protein's affinity to entrap water molecules in the structure reduces the water availability for ice crystallization in the frozen patties, thus reducing the water loss in the thawing process.<sup>44</sup> The milder cold plasma treatments at 170-15, 170-30, and 230-15 would cause a disturbance in the surface charge of the protein thereby causing partial aggregates. The

cold plasma-induced protein aggregates would have a better water-holding capacity thereby improving the water loss from the patty's structure.<sup>45</sup> However, under intense plasma processing conditions, the larger aggregates are further broken into smaller aggregates. The unstable and loose aggregates are reinforced by the development of additional covalent disulfide bonds. The rearrangement process of the protein aggregates makes the protein more permeable and thereby reduces the ability to hold the water leading to relatively higher syneresis loss.<sup>46,47</sup>

**3.7.2 Cooking loss and moisture retention of patties.** The cooking loss and moisture retention are the key parameters that affect the texture and mouthfeel of the patties after cooking. The impact on cooking loss and moisture retention is depicted in Fig. 7. The addition of cold plasma-treated oat protein improved the cooking loss and moisture retention in the patties as compared to the TVP-based patties. However, the cooking loss is relatively increased in the OP-230-15 sample as compared to other patty samples. This might be due to the higher initial moisture content of the patties which is supported by the

Table 7 Effect of cold plasma on the texture analysis of oat protein patties<sup>a</sup>

Sample	Hardness	Adhesiveness	Springiness	Cohesiveness	Gumminess	Chewiness	Resilience
TVP	795.16 ± 37.97 <sup>a,1</sup>	-0.78 ± 0.04 <sup>a,1</sup>	0.92 ± 0.01 <sup>a,1</sup>	0.82 ± 0.01 <sup>a,1</sup>	649.53 ± 39.12 <sup>a,1</sup>	595.68 ± 28.08 <sup>a,1</sup>	0.38 ± 0.00 <sup>a,1</sup>
Control	718.89 ± 3.17 <sup>a,1</sup>	-0.32 ± 0.00 <sup>b,2</sup>	0.68 ± 0.00 <sup>b,2</sup>	0.61 ± 0.03 <sup>b,2</sup>	439.14 ± 21.27 <sup>b,2</sup>	296.93 ± 12.61 <sup>b,2</sup>	0.24 ± 0.01 <sup>b,2</sup>
170-15	1202.57 ± 51.36 <sup>b,2</sup>	-0.27 ± 0.07 <sup>b,2</sup>	0.75 ± 0.01 <sup>c,3</sup>	0.68 ± 0.02 <sup>c,3</sup>	824.04 ± 58.83 <sup>b,2</sup>	622.52 ± 49.24 <sup>b,2</sup>	0.35 ± 0.01 <sup>b,3</sup>
170-30	866.98 ± 231.87 <sup>b,3</sup>	-0.46 ± 0.21 <sup>b,3</sup>	0.80 ± 0.01 <sup>c,4</sup>	0.67 ± 0.02 <sup>c,3</sup>	575.83 ± 140.64 <sup>b,2</sup>	458.65 ± 106.75 <sup>b,2</sup>	0.34 ± 0.03 <sup>b,4</sup>
230-15	743.91 ± 18.34 <sup>c,2</sup>	-0.06 ± 0.01 <sup>b,2</sup>	0.74 ± 0.00 <sup>d,3</sup>	0.66 ± 0.03 <sup>c,3</sup>	488.95 ± 11.52 <sup>b,2</sup>	362.20 ± 8.96 <sup>b,2</sup>	0.27 ± 0.01 <sup>c,3</sup>
230-30	1255.21 ± 141.74 <sup>c,3</sup>	-0.63 ± 0.00 <sup>b,3</sup>	0.75 ± 0.02 <sup>d,4</sup>	0.82 ± 0.01 <sup>c,3</sup>	649.53 ± 102.97 <sup>b,2</sup>	595.68 ± 90.85 <sup>b,2</sup>	0.38 ± 0.00 <sup>c,4</sup>

<sup>a</sup> The values having different alphabets in the superscripts are statistically significant corresponding to voltage while the values having different numerical alphabets are statistically significant corresponding to the treatment time.



highest water-holding capacity of  $99.41 \pm 0.16$  in the sample. The impact of higher water content is reflected in the moisture content measurement, calculated after cooking. This indicates that the cold plasma treatment under selected conditions (230-15) increased the water holding and water retention capacity which would support improved textural and sensorial attributes of the patties during storage and after cooking.

**3.7.3 Compression juice loss in cooked patties.** The compression juice loss is measured after cooking the patties and indicates the available fat and moisture content in the cooked patties. The juiciness is another desirable characteristic of the patties for improving the mouthfeel. The effect of cold plasma treatment and incorporation of oat protein is shown in Fig. 7. On the addition of oat protein, the untreated and treated sample considerably increased the compression juice loss, due to their ability to absorb and retain the water and oil in the patty structure. Higher compression juice loss was observed in the OP-control sample and OP-230-15 sample, indicating the availability of fluid in the matrix that supports a more desirable soft texture in patties. The lower juice loss is observed in the patties incorporated with other cold plasma-treated samples indicating the weaker ability of the oat protein to hold the oil and water during preparation and cooking, which might degrade the juiciness of the patties.

**3.7.4 Texture characteristics of cooked patties.** Studies on the textural characteristics of cooked patties are significant for understanding their sensory attributes. The impact of the addition of cold plasma-treated oat protein in patties is given in Table 7. The addition of oat protein significantly altered all the textural parameters. The hardness of the control and 230-15 patties reduced after cooking which might be due addition of plasma-treated oat protein which has better moisture absorption and retention properties.<sup>48</sup> The improved gelling properties of the treated oat protein support the formation of softer patties.<sup>26</sup> This is also supported by the water holding capacity% results of the control (99%) and 230-15 (99.41%) samples. In contrast, the 170-15 and 230-30 patty samples exhibited higher hardness, indicating poor hydration and water-holding properties. Similarly, the 230-15 samples showed the increased softness of the patties *via* springiness and resilience values. The other textural characteristics showed minimal changes with respect to the cold plasma treatment conditions, but the addition of both treated and control oat protein improved the textural characteristics of the oat patties.

## 4. Conclusion

This study provides critical insights into the effect of atmospheric pin-to-plate cold plasma treatment at the selected voltages (170 & 230 V) and exposure times (15 and 30 min) on the rheological and thermal properties of oat protein and its application in plant-based patties. Rheological analysis revealed a significant increase in intrinsic viscosity in both dispersion and gel forms, indicating enhanced protein hydration and structural modifications. The plasma-induced aggregation facilitated better visco-elastic behaviour with increased stability, as shown by the enhanced critical strain values. The

shear-thinning behavior of plasma-treated oat protein suggests improved dispersion and gelation properties, which are essential for forming stable and cohesive food matrices. The application of plasma-treated oat protein in plant-based patties demonstrated remarkable improvements in texture, firmness, and juiciness. The enhanced gelation and water-holding capacity contributed to better structural integrity, reducing cooking loss while maintaining a desirable mouthfeel. These modifications are crucial in mimicking the texture of conventional meat, making plasma-treated oat protein a promising ingredient for plant-based meat formulations. To conclude, oat proteins treated under 230-15 conditions showed desirable rheological and textural outcomes both as a protein gel and as a texturizer in plant-based patty applications. However, the desired functional properties of plant proteins can be tailored by altering the process parameters of cold plasma. By leveraging cold plasma technology, the food industry can develop functional plant proteins without chemical additives, aligning with the growing demand for clean-label and sustainable alternatives. Future research should focus on optimizing plasma treatment conditions for different food matrices and assessing their long-term effects on sensory attributes. Overall, this study highlights the potential of cold plasma treatment as an innovative approach to improving plant protein functionality, paving the way for high-quality, meat-like plant-based foods.

## Data availability

All the data obtained from the analysis in the present study are given in the form of figures and tables, attached as separate files in the manuscript.

## Conflicts of interest

The authors declare that there are no conflicts of interest

## References

- 1 S. Zhao, L. Wang, W. Hu and Y. Zheng, Meet the meatless: demand for new generation plant-based meat alternatives, *Appl. Econ. Perspect. Pol.*, 2023, **45**(1), 4–21.
- 2 *Plant-based Protein Industry worth \$20.5 billion by 2029, 2024*, available from: <https://www.marketsandmarkets.com/PressReleases/plant-based-protein.asp>.
- 3 U. Holopainen-Mantila, S. Vanhatalo, P. Lehtinen and N. Sozer, Oats as a source of nutritive alternative protein, *J. Cereal Sci.*, 2024, **116**, 103862.
- 4 R. Li and Y. L. Xiong, Sensitivity of oat protein solubility to changing ionic strength and pH, *J. Food Sci.*, 2021, **86**(1), 78–85.
- 5 M. Ibrahim, A. Aav and I. Jöodu, The potential and limitations for applications of oat proteins in the food industry, *Agron. J.*, 2022, **20**(1), 161–173.
- 6 U. S. Annapure and T. K. Ranjitha Gracy, Plasma modification, in *Physicochemical and Enzymatic Modification of Gums: Synthesis, Characterization and Application*,

Springer International Publishing, Cham, 2022, vol. 8, pp. 193–211.

- 7 A. Dabade, S. Kahar, A. Acharjee, P. Bhushette and U. Annapure, Effect of atmospheric pressure non-thermal pin to plate cold plasma on structural and functional properties of soy protein isolate, *J. Agric. Food Res.*, 2023, **12**, 100538.
- 8 S. Zhang, W. Huang, E. Feizollahi, M. S. Roopesh and L. Chen, Improvement of pea protein gelation at reduced temperature by atmospheric cold plasma and the gelling mechanism study, *Innovative Food Sci. Emerging Technol.*, 2021, **67**, 102567.
- 9 H. Ji, S. Dong, F. Han, Y. Li, G. Chen, L. Li and Y. Chen, Effects of dielectric barrier discharge (DBD) cold plasma treatment on physicochemical and functional properties of peanut protein, *Food Bioprocess Technol.*, 2018, **11**, 344–354.
- 10 G. Eazhumalai, R. G. Kalaivandan and U. S. Annapure, Effect of atmospheric pin-to-plate cold plasma on oat protein: structural, chemical, and foaming characteristics, *Int. J. Biol. Macromol.*, 2023, **242**, 125103.
- 11 J. O'sullivan, B. Murray, C. Flynn and I. Norton, The effect of ultrasound treatment on the structural, physical and emulsifying properties of animal and vegetable proteins, *Food Hydrocoll.*, 2016, **53**, 141–154.
- 12 R. G. Kalaivandan, G. Eazhumalai and U. S. Annapure, Impact of pin-to-plate cold plasma depolymerization on the gelation and functional attributes of guar galactomannan, *J. Food Process. Eng.*, 2023, **46**(7), e14340.
- 13 A. Daerr and A. Mogne, Pendent\_drop: an imagej plugin to measure the surface tension from an image of a pendent drop, *J. Open Res. Software*, 2016, **4**(1), e3.
- 14 S. Zhang, W. Huang, E. Feizollahi, M. S. Roopesh and L. Chen, Improvement of pea protein gelation at reduced temperature by atmospheric cold plasma and the gelling mechanism study, *Innovative Food Sci. Emerging Technol.*, 2021, **67**, 102567.
- 15 J. K. Joy, R. G. Kalaivandan, G. Eazhumalai, S. P. Kahar and U. S. Annapure, Effect of pin-to-plate atmospheric cold plasma on jackfruit seed flour functionality modification, *Innovative Food Sci. Emerging Technol.*, 2022, **78**, 103009.
- 16 T. V. Nieto-Nieto, Y. X. Wang, L. Ozimek and L. Chen, Effects of partial hydrolysis on structure and gelling properties of oat globular proteins, *Food Res. Int.*, 2014, **55**, 418–425.
- 17 Y. Shen, S. Hong, Z. Du, M. Chao, T. O'Quinn and Y. Li, Effect of adding modified pea protein as functional extender on the physical and sensory properties of beef patties, *LWT-Food Sci. Technol.*, 2022, **154**, 112774.
- 18 M. A. Masuelli and M. G. Sansone, Hydrodynamic properties of gelatin-studies from intrinsic viscosity measurements, *Prod. Appl. Biopolym.*, 2012, 85–116.
- 19 R. Curvale, M. Masuelli and A. P. Padilla, Intrinsic viscosity of bovine serum albumin conformers, *Int. J. Biol. Macromol.*, 2008, **42**(2), 133–137.
- 20 R. Pamies, J. G. Hernández Cifre, M. del Carmen López Martínez and J. García de la Torre, Determination of intrinsic viscosities of macromolecules and nanoparticles. Comparison of single-point and dilution procedures, *Colloid Polym. Sci.*, 2008, **286**, 1223–1231.
- 21 S. Dong, P. Guo, Y. Chen, G. Y. Chen, H. Ji, Y. E. Ran, S. H. Li and Y. E. Chen, Surface modification via atmospheric cold plasma (ACP): improved functional properties and characterization of zein film, *Ind. Crops Prod.*, 2018, **115**, 124–133.
- 22 A. Gomes and P. J. Sobral, Plant protein-based delivery systems: an emerging approach for increasing the efficacy of lipophilic bioactive compounds, *Molecules*, 2021, **27**(1), 60.
- 23 A. Segat, N. N. Misra, P. J. Cullen and N. Innocente, Atmospheric pressure cold plasma (ACP) treatment of whey protein isolate model solution, *Innovative Food Sci. Emerging Technol.*, 2015, **29**, 247–254.
- 24 L. Tan, X. Hua, L. Yin, X. Jia and H. Liu, Effect of corona discharge cold plasma on the structure and emulsification properties of soybean protein isolate, *Food Hydrocoll.*, 2024, **156**, 110337.
- 25 S. Savadkoohi and A. Farahnaky, Dynamic rheological and thermal study of the heat-induced gelation of tomato-seed proteins, *J. Food Eng.*, 2012, **113**(3), 479–485.
- 26 S. Zhang, W. Huang, M. S. Roopesh and L. Chen, Pre-treatment by combining atmospheric cold plasma and pH-shifting to prepare pea protein concentrate powders with improved gelling properties, *Food Res. Int.*, 2022, **154**, 111028.
- 27 C. Y. Ma and V. R. Harwalkar, Chemical characterization and functionality assessment of oat protein fractions, *J. Agric. Food Chem.*, 1984, **32**(1), 144–149.
- 28 S. Braspaiboon, S. Osiriphun, P. Peepathum and W. Jirarattanarangsri, Comparison of the effectiveness of alkaline and enzymatic extraction and the solubility of proteins extracted from carbohydrate-digested rice, *Heliyon*, 2020, **6**(11), e05403.
- 29 N. S. Kumar, A. H. Dar, K. K. Dash, B. Kaur, V. K. Pandey, A. Singh, U. Fayaz, R. Shams, S. A. Mukarram and B. Kovács, Recent advances in cold plasma technology for modifications of proteins: a comprehensive review, *J. Agric. Food Res.*, 2024, **25**, 101177.
- 30 N. Mollakhalili-Meybodi, M. Yousefi, A. Nematollahi and N. Khorshidian, Effect of atmospheric cold plasma treatment on technological and nutrition functionality of protein in foods, *Eur. Food Res. Technol.*, 2021, **247**, 1579–1594.
- 31 A. Acharjee, A. Dabade, S. Kahar and U. Annapure, Effect of atmospheric pressure non-thermal pin to plate cold plasma on structural and functional properties of pea protein isolate, *J. Agric. Food Res.*, 2023, **14**, 100821.
- 32 M. Laitinen, T. Kokkonen, X. Huang, K. Jouppila, N. H. Maina and N. Mäkelä-Salmi, Gelation potential of oat protein isolate: influence of extraction method, gelling conditions, and enzymatic modification, *Food Chem.*, 2025, **481**, 143968.
- 33 S. Santinath Singh, V. K. Aswal and H. B. Bohidar, Internal structures of agar-gelatin co-hydrogels by light scattering,



small-angle neutron scattering and rheology, *Eur. Phys. J. E:Soft Matter Biol. Phys.*, 2011, **34**(6), 62.

34 O. O. Olatunde, A. Hewage, T. Dissanayake, R. E. Aluko, A. C. Karaca, N. Shang and N. Bandara, Cold atmospheric plasma-induced protein modification: novel nonthermal processing technology to improve protein quality, functionality, and allergenicity reduction, *Compr. Rev. Food Sci. Food Saf.*, 2023, **22**(3), 2197–2234.

35 J. E. Martín-Alfonso, A. A. Cuadri, M. Berta and M. Stading, Relation between concentration and shear-extensional rheology properties of xanthan and guar gum solutions, *Carbohydr. Polym.*, 2018, **181**, 63–70.

36 M. Kloot, C. Brzeski and S. Drusch, Effect of protein aggregation on rheological properties of pea protein gels, *Food Hydrocoll.*, 2020, **108**, 106036.

37 M. Dharini, S. Jaspin and R. Mahendran, Cold plasma reactive species: generation, properties, and interaction with food biomolecules, *Food Chem.*, 2023, **405**, 134746.

38 H. Tolouie, M. A. Mohammadifar, H. Ghomi and M. Hashemi, Cold atmospheric plasma manipulation of proteins in food systems, *Crit. Rev. Food Sci. Nutr.*, 2018, **58**(15), 2583–2597.

39 H. M. Mehr and A. Koocheki, Effects of short-term and long-term cold plasma treatment on the color, structure, and Pickering foaming properties of Grass pea protein particles, *Food Hydrocoll.*, 2023, **143**, 108846.

40 H. Ji, S. Dong, F. Han, Y. Li, G. Chen, L. Li and Y. Chen, Effects of dielectric barrier discharge (DBD) cold plasma treatment on physicochemical and functional properties of peanut protein, *Food Bioprocess Technol.*, 2018, **11**, 344–354.

41 A. H. Clark, G. M. Kavanagh and S. B. Ross-Murphy, Globular protein gelation—theory and experiment, *Food Hydrocoll.*, 2001, **15**(4–6), 383–400.

42 M. M. Rahman and B. P. Lamsal, Effects of atmospheric cold plasma and high-power sonication on rheological and gelling properties of mung bean protein dispersions, *Food Res. Int.*, 2023, **163**, 112265.

43 C. Yang, Y. Wang and L. Chen, Fabrication, characterization and controlled release properties of oat protein gels with percolating structure induced by cold gelation, *Food Hydrocoll.*, 2017, **62**, 21–34.

44 L. Mirmoghtadaie, M. Kadivar and M. Shahedi, Effect of modified oat starch and protein on batter properties and quality of cake, *Cereal Chem.*, 2009, **86**(6), 685–691.

45 Y. Ma and F. Chen, Plant protein heat-induced gels: Formation mechanisms and regulatory strategies, *Coatings*, 2023, **13**(11), 1899.

46 A. C. Alting, R. J. Hamer, C. G. de Kruif and R. W. Visschers, Cold-set globular protein gels: Interactions, structure and rheology as a function of protein concentration, *J. Agric. Food Chem.*, 2003, **51**(10), 3150–3156.

47 P. Roccia, P. D. Ribotta, G. T. Pérez and A. E. León, Influence of soy protein on rheological properties and water retention capacity of wheat gluten, *LWT–Food Sci. Technol.*, 2009, **42**(1), 358–362.

48 S. Hong, Y. Shen and Y. Li, Physicochemical and functional properties of texturized vegetable proteins and cooked patty textures: comprehensive characterization and correlation analysis, *Foods*, 2022, **11**(17), 2619.

